Differential Cytotoxic Responses to Low- and High-Dose Photodynamic Therapy in Human Gastric and Bladder Cancer Cells

Je-Ok Yoo, Young-Cheol Lim, Young-Myeong Kim, and Kwon-Soo Ha*

Department of Molecular and Cellular Biochemistry, School of Medicine, Kangwon National University, Chuncheon, Kangwon-do 200-701, Korea

ABSTRACT

Here, we present differential cytotoxic responses to two different doses of photodynamic therapies (PDTs; low-dose PDT [LDP] and high-dose PDT [HDP]) using a chlorin-based photosensitizer, DH-II-24, in human gastric and bladder cancer cells. Fluorescence-activated cell sorting analysis using Annexin V and propidium iodide (PI) showed that LDP induced apoptotic cell death, whereas HDP predominantly caused necrotic cell death. The differential cytotoxic responses to the two PDTs were further confirmed by a $DiOC_6$ and PI double-staining assay via confocal microscopy. LDP, but not HDP, activated caspase-3, which was inhibited by Z-VAD, Trolox, and BAPTA-AM. LDP and HDP demonstrated opposite effects on intracellular reactive oxygen species (ROS)/Ca^{2+} signals; LDP stimulated intracellular ROS production, contributing to a transient increase of intracellular Ca^{2+}, whereas HDP induced a massive and prolonged elevation of intracellular Ca^{2+} responsible for the transient production of intracellular ROS. In addition, the two PDTs also increased in situ transglutaminase 2 (TG2) activity, with a higher stimulation by HDP, and this increase in activity was prevented by Trolox, BAPTA-AM, and TG2-siRNA. LDP-induced apoptotic cell death was strongly inhibited by Trolox and TG2-siRNA and moderately suppressed by BAPTA-AM. However, HDP-mediated necrotic cell death was partially inhibited by BAPTA-AM but not by TG2-siRNA. Thus, these results demonstrate that LDP and HDP induced apoptotic and necrotic cell death by differential signaling mechanisms involving intracellular Ca^{2+}, ROS, and TG2. J. Cell. Biochem. 112: 3061–3071, 2011. © 2011 Wiley-Liss, Inc.

KEY WORDS: PHOTODYNAMIC THERAPY; CELL DEATH, TISSUE TRANSGLUTAMINASE; REACTIVE OXYGEN SPECIES; INTRACELLULAR Ca^{2+}

Photodynamic therapy (PDT) has been increasingly recognized as a selective treatment modality for various cancers and diseases [Triesscheijn et al., 2006; Lim et al., 2009; O'Connor et al., 2009; Robertson et al., 2009; Bredell et al., 2010]. Although an enormous number of studies have reported that PDT can induce many cellular and molecular signaling events that ultimately result in cell death, we remain far from a definitive understanding of the mechanisms of tumor cell killing because the efficiency and specific mechanism(s) of cell death are largely determined by a variety of parameters such as the concentration and intracellular localization of the photosensitizer, dose of light, cell genotype, and oxygen availability [Sharman et al., 1999; Nowis et al., 2005; Triesscheijn et al., 2006; Robertson et al., 2009]. The action mechanism of PDT is usually based on the production of reactive oxygen species (ROS) such as singlet oxygen and free radicals, which may cause cell death by apoptosis and/or necrosis. Although cell death resulting from PDT is triggered mostly by ROS, it is also regulated by intracellular Ca^{2+} events [Almeida et al., 2004; Buytaert et al., 2007]. Moreover, massive production of intracellular ROS and Ca^{2+} overload may trigger a shift from apoptosis to necrosis [Buytaert

et al., 2007]. Thus, increases in intracellular ROS and/or Ca^{2+} concentrations due to PDT may result in the induction of apoptosis or necrosis, although the regulation mechanism remains to be explored.

Transglutaminase 2 (TG2, tissue transglutaminase) is a member of the transglutaminase family. TG2 catalyzes transamidation reactions resulting in the formation of the ε-(γ-glutamyl)lysine or (γ-glutamyl)-polyamine bonds in a Ca^{2+}-dependent manner, and these reactions are regulated by various factors including nitric oxide, sphingosylphosphocholine, UV, oxidative stress, Ca^{2+}, and GTP [Griffin et al., 2002; Yi et al., 2004; Yoo et al., 2005; Park et al., 2010]. TG2 is a multifunctional protein that is implicated in regulating several physiological processes such as cell death, cell adhesion and differentiation, survival, cell migration, and oocyte maturation [Kim et al., 2001; Fok and Mehta, 2007; Mangala et al., 2007; Ruan et al., 2007; Park et al., 2010]. Beyond its functional variety, TG2 exerts both pro- and antiapoptotic effects [Fok and Mehta, 2007; Robitaille et al., 2008]. Interestingly, it has been demonstrated that the regulatory mechanism of cell death by TG2 is dependent on several parameters, such as stimulus, mediator, and cell type [Tucholski and Johnson, 2002; Ruan et al., 2007; Park et al., 2010; Tee et al., 2010]. However, the biological role of TG2 in PDT-induced cell death remains to be clearly defined.

In the present study, we comparatively analyzed differential cytotoxic responses to PDT with DH-II-24, a chlorin-based photosensitizer, in human gastric and bladder cancer cells. Recently, we investigated the in vivo antitumor effects of PDT with DH-II-24, which exhibits several advantages such as strong absorption at relatively long wavelengths, minimal dark toxicity, and a shorter half-life in the body [Lim et al., 2009, 2011]. Our results demonstrate that DH-II-24-mediated PDT could induce cell death through both apoptosis and necrosis in a PDT dose-dependent manner; intracellular ROS play a decisive role in the TG2-dependent apoptotic cell death induced by low-dose PDT (LDP), whereas high-dose PDT (HDP)-mediated necrotic cell death is controlled dominantly by intracellular Ca^{2+} overload.

MATERIALS AND METHODS

CELL CULTURE AND CHEMICALS
AGS (human gastric adenocarcinoma) and J82 (human bladder carcinoma) cells (ATCC, Manassas, VA) were studied because TG2 is expressed in two cancer cell lines [Yoo et al., 2005; Kwon et al., 2009]. AGS and J82 cells were maintained at $37°C$ in RPMI 1640 medium supplemented with 10% FBS, 100 U/ml penicillin, and 100 μg/ml streptomycin (culture medium) in a 5% CO_2 atmosphere. MitoTracker Green FM, LysoTracker Green DND-26, $DiOC_6$(3), H_2DCFDA, and Fluo 4-AM were obtained from Molecular Probes (Carlsbad, CA). Z-VAD-fmk was purchased from Alexis Biochemicals (San Diego, CA). 5-(Biotinamido)pentylamine and FITC-conjugated streptavidin were obtained from Pierce (Rockford, IL). DH-II-24 (methyl-13^b-(2-dimethylaminoethoxycarbonyl)-13^b-demethoxycarbonyl-pheophorbide α) was kindly provided by Professor Chang-Hee Lee (Department of Chemistry, Kangwon National University, Korea).

PDT USING AN ON-STAGE SYSTEM
To perform real-time photoactivation and monitoring of cellular responses in the same environment, an on-stage system was assembled by installing a long-pass filter (LP630, Fiber Optic Korea, Korea) in the filter holder of the illumination column of a confocal microscope (FV300, Olympus, Japan).

In preparation for PDT, cells grown on round coverslips or in culture plates were incubated for 12 h under darkness with 1 or 5 μg/ml DH-II-24 for LDP or HDP, respectively, in culture medium. After washing twice with the culture medium, coverslips were mounted onto a perfusion chamber (Seoul Engineering, Korea), and the perfusion chamber or culture plates were placed on the microscope stage of the confocal microscope at a distance of 5 cm from the condenser. The photosensitizer-loaded cells were irradiated at $1.45\,mW/cm^2$ for 15 (21.8 mJ/cm^2), 30 (43.5 mJ/cm^2), 60 (87.0 mJ/cm^2, LDP), 90 (130.5 mJ/cm^2, HDP), or 120 s (174.0 mJ/cm^2) under darkness by the built-in 100-W halogen lamp. Sometimes, cells were treated with various inhibitors for 30 min before PDT, at $37°C$ in culture medium.

UPTAKE AND LOCALIZATION OF DH-II-24
To measure uptake of DH-II-24, cells were grown on round coverslips and incubated for 12 h with various concentrations of DH-II-24 in culture medium. The loaded cells were observed under the confocal microscope with a 543 HeNe laser and a 565 longpass filter. Approximately 30 cells were randomly selected from three independent experiments, and the fluorescence intensities were determined at a single cell level.

To localize DH-II-24, cells grown on round coverslips were loaded for 12 h with 5 μg/ml of DH-II-24 in culture medium, and then incubated, in culture medium, with 200 nM MitoTracker Green FM for 30 min, 1 μM LysoTracker Green DND-26 for 10 min, or 400 nM $DiOC_6$(3) for 20 min to label mitochondria, lysosomes, and ER, respectively. The stained live cells were observed by confocal microscopy.

FACS ANALYSIS
At 4 h after PDT, cells were harvested, resuspended in PBS (1×10^6 cells/ml), and incubated under darkness at $4°C$ for 15 min with 20-fold diluted Annexin V-FITC and 10 μg/ml propidium iodide (PI) in the binding buffer, according to the manufacturer's instructions (BD Biosciences, San Diego, CA). Stained cells were analyzed using a FACScan flow cytometer (Becton Dickinson, Mountain View, CA), and at least 10,000 events were collected for each sample.

$DiOC_6$ AND PI DOUBLE-STAINING ASSAY
The type of cell death was determined by $DiOC_6$/PI double-staining using a confocal microscope, by a modification of the procedures of Douma et al. [2004]. Briefly, after PDT, cells were co-treated with 50 nM 3,3'-dihexyloxacarbocyanine iodide ($DiOC_6$) and 10 μg/ml PI at $37°C$ for 20 min in culture medium. Stained cells were analyzed by confocal microscopy (FV300). Viable, apoptotic, and necrotic cells were characterized by high $DiOC_6$ and low PI fluorescence, low $DiOC_6$ and PI fluorescence, and low $DiOC_6$ and high PI fluorescence, respectively. Approximately 60 cells were randomly selected for the control, LDP, and HDP treatments, and the fluorescence intensities

of PI and DiOC$_6$ were determined at the single-cell level. The results were normalized by the average intensity of the control cells and expressed as the relative fluorescence intensity (RFI).

IN VITRO CASPASE–3 ACTIVITY ASSAY

Cells were incubated for 30 min with lysis buffer (50 mM HEPES, pH 7.5, 1% Triton X-100, 10% glycerol, 150 mM NaCl, and 1 mM EDTA), scraped off, and centrifuged at 20,000g for 10 min at 4°C. Then, the soluble fraction of cell lysate was incubated for 1 h at 37°C with 100 μM Ac-DEVD-pNA (colorimetric substrate for caspase-3: Ac-Asp-Glu-Val-Asp-pNA), according to the manufacturer's instructions (Alexis Biochemicals). The absorbance of each sample was read at 405 nm using a microplate reader (Molecular Device, Sunnyvale, CA).

MEASUREMENT OF INTRACELLULAR ROS

The level of intracellular ROS was determined using the on-stage system, according to the procedures of Lee et al. [2003]. Briefly, cells grown on round coverslips were loaded with DH-II-24 for 12 h and incubated with 10 μM H$_2$DCFDA for 10 min in culture medium lacking phenol red. The labeled cells were mounted and immediately irradiated on perfusion chambers with the built-in halogen lamp. Following incubation for the desired times, the level of intracellular ROS was determined by confocal microscopy. The cells were excited by a 488 nm argon laser, and images were filtered by a bandpass filter (BP 510–530 nm). Approximately 30 cells were randomly selected from three independent experiments, and fluorescence intensities of the cells were determined at the single-cell level using the Fluoview software of the confocal microscope (Olympus). The level of intracellular ROS was determined by comparing the fluorescence intensities of irradiated cells with those of non-irradiated control cells (fold).

MONITORING OF INTRACELLULAR Ca^{2+}

Changes in the levels of intracellular Ca^{2+} were monitored using the on-stage system. Cells on round coverslips were loaded with DH-II-24 for 12 h in culture medium and incubated with 2 μM Fluo 4-AM for 30 min. Coverslips were mounted on the perfusion chamber and scanned every 60 s by confocal microscopy with a 488-nm excitation argon laser and a 510-nm longpass emission filter. At the indicated times during scanning, the cells were irradiated with the built-in halogen lamp. Serial images from the scanning were processed to analyze changes in intracellular Ca^{2+} at the single-cell level. The results were expressed as the RFI.

TRANSFECTION OF SMALL INTERFERING RNA

Cells were transfected with TG2-small interfering RNA (siRNA) according to the procedures of Yi et al. [2004]. Briefly, TG2-siRNA duplex, 5′-AAGAGCGAGAUGAUCUGGAAC-3′ was synthesized to target the coding sequence of human TG2 mRNA (Dharmacon, Lafayette, CO). Cells were transfected with siRNAs using siLent-Fect^{TM} Lipid Reagent (Bio-Rad) according to the manufacturer's instructions. At 20 h after transfection, the medium was replaced with fresh culture medium and the transfected cells were incubated for further 24 h prior to use in experiments.

MEASUREMENT OF IN SITU TG2 ACTIVITY BY CONFOCAL MICROSCOPY

In situ TG2 activity was determined by a confocal microscopic assay according to the procedures of Lee et al. [2003]. Briefly, DH-II-24-loaded cells were incubated with 1 mM 5-(biotinamido)pentylamine (a pseudosubstrate of TG2) for 1 h at 37°C, and irradiated with the built-in halogen lamp. The irradiated cells were fixed with 3.7% formaldehyde in PBS for 30 min and permeabilized with 0.2% Triton X-100 in PBS for 30 min at room temperature. Following incubation with a blocking solution (2% BSA in TBS containing 0.1% Tween 20), the cells were treated with FITC-conjugated streptavidin (1: 200, v/v) in the blocking solution for 1 h and observed under the confocal microscope. Approximately 30 cells were randomly selected from three separate experiments, and their fluorescence intensities were determined by processing their FITC-images at a single-cell level. TG2 activity was determined by comparing the fluorescence intensities of treated cells with those of untreated control cells (fold).

CELL VIABILITY ASSAY

Cell viability was measured by the 3-(4,5-dimethylthiazol-2-yl)-2,5-diphenyltetrazolium bromide (MTT) assay. Cells were incubated with DH-II-24 in 24-well culture plates and irradiated with the built-in halogen lamp. At 24 h after irradiation, the cells were incubated with 1 mg/ml MTT solution for 4 h at 37°C, and the resulting insoluble purple formazan crystal was dissolved in isopropanol. The absorbance at 570 nm was measured using the microplate reader and cell viability was expressed as a percentage of that for nonirradiated control cells.

STATISTICAL ANALYSIS

Data are expressed as means ± S.D. Statistical significance was analyzed using one-way analysis of variance (ANOVA) (Origin 6.1 software from OriginLab Corp., Northampton, MA), and a P-value of 0.05 or less was considered statistically significant.

RESULTS

UPTAKE AND SUBCELLULAR LOCALIZATION OF DH–II–24

We initially studied the uptake of DH-II-24 in AGS cells by confocal microscopy. The absorption spectrum and chemical structure of the chlorin-based photosensitizer are shown in Figure 1A. Cells were incubated with various concentrations of DH-II-24 for 12 h and the uptake was determined at the single-cell level by confocal microscopy. As shown in Figure 1B, cells became loaded with DH-II-24 in a dose-dependent manner, with maximal uptake at 5 μg/ml. To investigate the subcellular localization of DH-II-24, AGS cells were loaded with DH-II-24 for 12 h and incubated with intracellular organelle-specific fluorophores to label mitochondria, lysosomes, and ER, respectively. The stained live cells were observed by confocal microscopy (Fig. 1C), and merged images and fluorescence intensity line profiling revealed that DH-II-24 colocalized well with DiOC$_6$(3) and moderately with MitoTracker Green and LysoTracker Green, demonstrating that DH-II-24 accumulated in the ER and to a lesser extent in mitochondria and lysosomes.
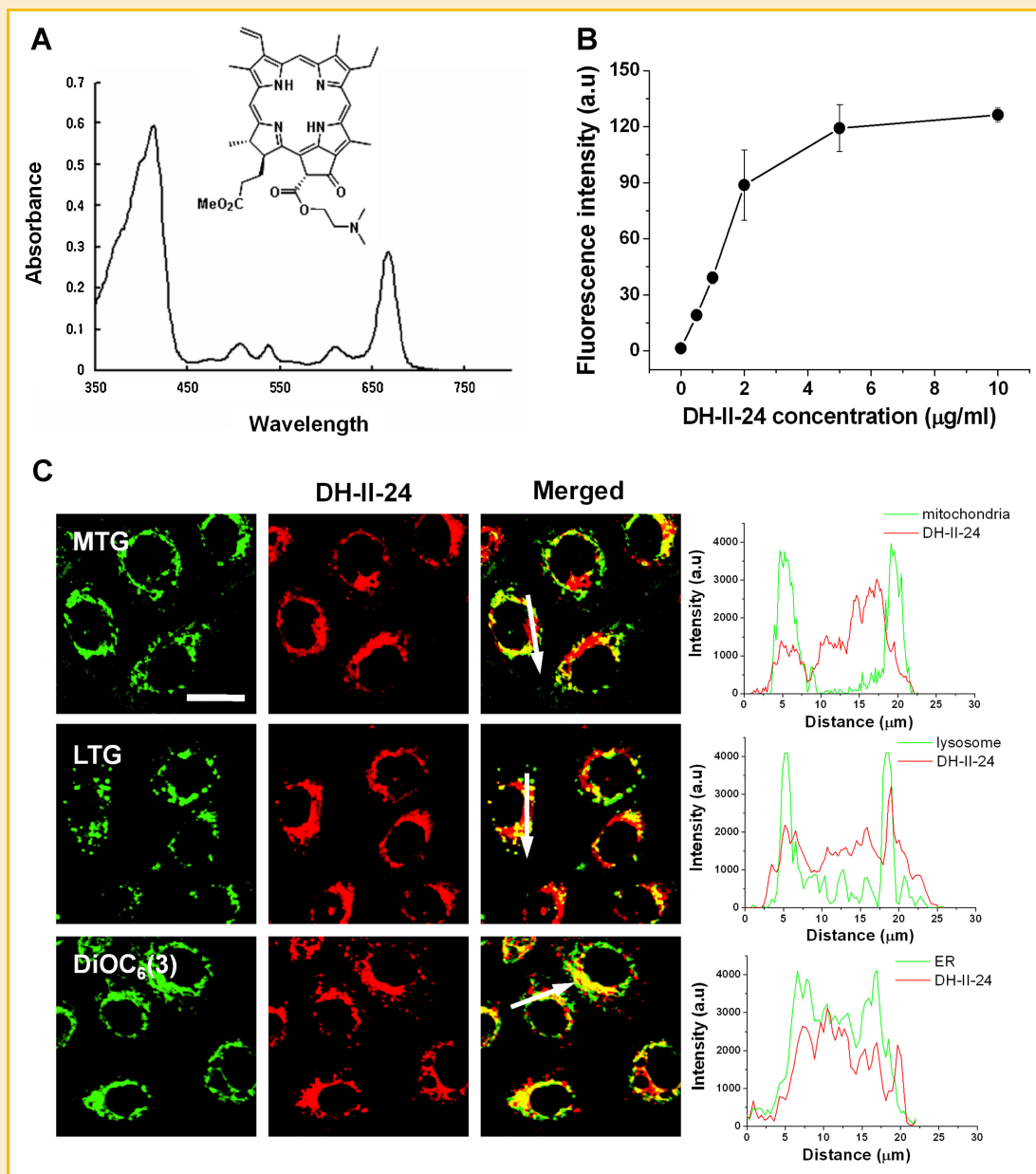
Fig. 1. Dose–dependent uptake and subcellular localization of DH–II–24 in AGS cells. A: The visible absorption spectrum of DH–II–24 with a predominant Q–band absorption at 666 nm. B: AGS cells grown on round coverslips were incubated with the indicated concentrations of DH–II–24 for 12 h, and the uptake of DH–II–24 was determined at the single–cell level by confocal microscopy as described in the Materials and Methods section. Values in graphs represent means ± S.D. from three independent experiments. C: DH–II–24–loaded (red) AGS cells were labeled with intracellular organelle probes (green), MitoTracker Green FM (MTG), LysoTracker Green DND-26 (LTG), and DiOC$_6$(3), and observed by confocal microscopy. Bar, 20 μm. Fluorescence intensity line profiles of DH–II–24 (red lines) and organelle probes (green lines) were obtained by scanning the merged images along the arrows. [Color figure can be seen in the online version of this article, available at http://wileyonlinelibrary.com/journal/jcb]

DIFFERENTIAL CYTOTOXIC RESPONSES TO LDP AND HDP

As it is known that PDT-induced cell death depends on the photosensitizer concentration and the light dose, we loaded AGS cells with 1 or 5 μg/ml of DH-II-24 for 12 h, and evaluated cell viability at 24 h after exposing cells to various light doses. As shown in Figure 2A, cell viability dramatically decreased in a light dose-dependent manner, with a half-maximal effect at 1 μg/ml DH-II-24 and 87 mJ/cm^2 light dose, and with a severe effect (less than 10% viability) at 5 μg/ml DH-II-24 and 130.5 mJ/cm^2 light dose. Two doses of PDT were chosen as treatment conditions for LDP and HDT, respectively. However, either DH-II-24 alone or light alone had little effect on cell viability.

Next, we exposed AGS cells to LDP and HDP, and investigated the type of cell death induced after staining with Annexin V-FITC and PI. LDP and HDP induced different modes of cell death; LDP induced apoptotic cell death, whereas HDP predominantly caused necrotic cell death (Fig. 2B and C). The mode of cell death was supported by a DiOC$_6$ and PI double-staining assay. DiOC$_6$ has been used as an
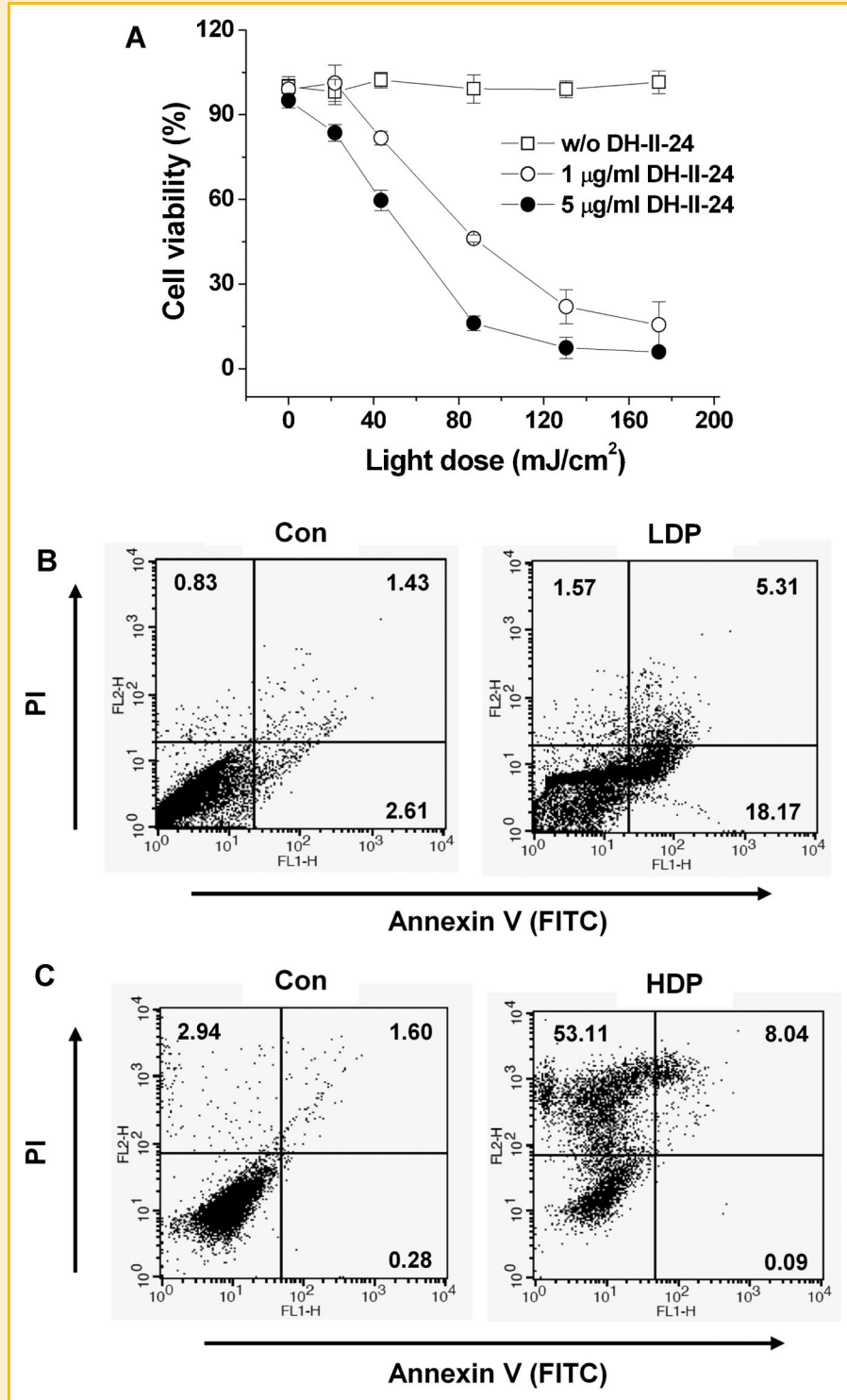
Fig. 2. Differential cytotoxic responses to LDP and HDP. AGS cells were loaded with 1 or 5 µg/ml DH–II–24 for 12 h and irradiated for various times. A: A light dose–dependent death of cells loaded with 1 or 5 µg/ml DH–II–24. B and C: Cells were stained with Annexin V/PI as described in the Materials and Methods section, and then analyzed using a FACScan flow cytometer 4 h after LDP or HDP. The left lower quadrant represents live cells, the right lower quadrant contains apoptotic cells, and the upper left includes necrotic cells. D: Cells were stained with $DiOC_6$ and PI, and the fluorescence intensity was measured by processing images at the single–cell level using confocal microscopy. E: DH–II–24–loaded cells were treated with 100 µM Z–VAD–fmk (Z–VAD), 5 mM Trolox, or 10 µM BAPTA–AM (BAPTA) for 30 min at 37°C in culture medium, and in vitro caspase–3 activity was determined at 4 h after PDT. LDP–induced activation of caspase–3 was inhibited by Z–VAD–fmk, Trolox, and BAPTA–AM, whereas HDP had no significant effect on caspase–3 activity. Values in graphs represent means ± S.D. from three independent experiments.
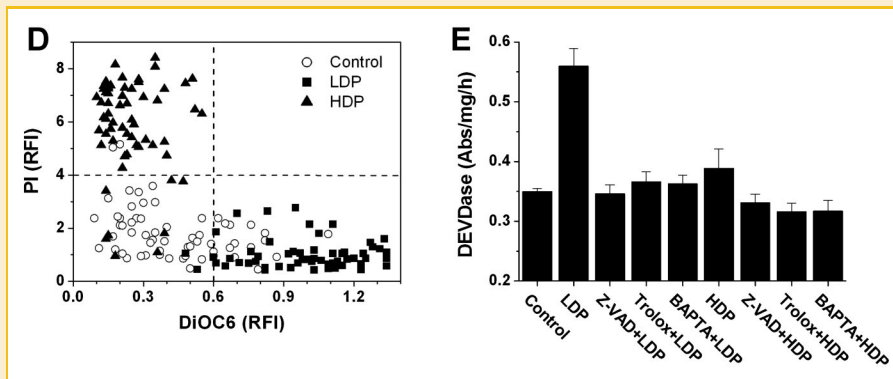
Fig. 2. (Continued)

apoptosis-dependent fluorophore [Douma et al., 2004]. Cells distributed into three populations (Fig. 2D). In the control condition, cells were viable (high $DiOC_6$ and low PI fluorescence). LDP-treated cells were mostly in the apoptotic population (low DiOC6 and PI), whereas the necrotic population was highly populated by HDP-treated cells (low DiOC6 and high PI). Moreover, we measured caspaes-3 activity as an indicator of apoptosis (Fig. 2E). LDP significantly activated caspase-3, suggesting that it may induce apoptotic cell death through a caspase-dependent pathway. As expected, the activation was completely inhibited by not only a broad-spectrum caspase inhibitor, Z-VAD-fmk, but also by an ROS scavenger, Trolox, and an intracellular Ca^{2+} chelator, BAPTA-AM, intimating that ROS and Ca^{2+} are related to LDP-induced apoptotic cell death. In contrast, HDP had no significant effect on caspase-3 activity. Thus, LDP induced apoptotic cell death by mechanism(s) involving caspase-3, whereas HDP caused necrotic cell death by caspase-independent mechanism(s).

CHANGES IN THE LEVELS OF INTRACELLULAR ROS AND Ca^{2+} INDUCED BY LDP AND HDP

PDT with most photosensitizers, in the presence of molecular oxygen, causes the generation of intracellular ROS including primarily singlet oxygen, hydroxyl radicals, and superoxide anions [Almeida et al., 2004; Buytaert et al., 2007]. Thus, we investigated the production of intracellular ROS in AGS cells treated by LDP or HDP. As shown in Figure 3A, LDP induced the production of intracellular ROS, with the maximum increase observed at 40 min after irradiation, followed by a slow decrease in the ROS level over 50 min. Conversely, HDP induced a rapid increase in intracellular ROS, with a maximal increase observed at 20 min after irradiation, followed by a prompt decrease to the basal level. Thus, LDP and HDP induced a similar maximal increase (approximately twofold) in intracellular ROS production at different post-irradiation times. However, LDP induced a sustained increase of intracellular ROS for a longer time than HDP, suggesting that intracellular ROS may mediate the cytotoxic events induced by LDP.

As it has been reported that PDT elevates intracellular Ca^{2+} levels in tumor cells [Buytaert et al., 2006; Lu et al., 2006], we examined changes in intracellular Ca^{2+} levels induced by LDP and HDP. As shown in Figure 3B, LDP induced a rapid increase in the level of intracellular Ca^{2+}, which promptly returned to the basal level. HDP also rapidly increased intracellular Ca^{2+} levels with a higher intensity than LDP, and the elevated Ca^{2+} level maintained for at least 30 min, implying that increased level of intracellular Ca^{2+} may contribute to HDP-induced cell death. Taken together, these results suggest that increased levels of intracellular ROS and Ca^{2+}, sustained over time, may play important roles in the phototoxic response to LDP and HDP, respectively.

OPPOSITE EFFECTS OF LDP AND HDP ON INTRACELLULAR ROS AND Ca^{2+} SIGNALS

Next, we investigated the signaling pathway(s) responsible for the cytotoxic responses to LDP and HDP. As LDP and HDP with DH-II-24 induced differential changes in intracellular ROS and Ca^{2+} levels, respectively, in AGS cells (Fig. 3A and B), we investigated their reciprocal roles in changes in intracellular ROS and Ca^{2+} levels induced by the two doses of PDT. We incubated cells with Trolox and BAPTA-AM and studied their effects on the LDP- or HDP-induced changes in intracellular Ca^{2+} and ROS levels. BAPTA-AM had no inhibitory effect on the production of ROS induced by LDP, whereas Trolox partially but significantly inhibited LDP-induced increase in Ca^{2+} levels (Fig. 3C and D), demonstrating that ROS production contributed to the elevation of intracellular Ca^{2+} levels in response to LDP. Contrary to these results, the HDP-induced production of intracellular ROS was completely blocked by BAPTA-AM, but Trolox did not affect the increase in Ca^{2+} levels induced by HDP (Fig. 3C and D), in consistent with a previous report [Yoo et al., 2009], suggesting that the elevation of Ca^{2+} resulted in the production of ROS in response to HDP. Thus, these results support the suggestion that sustained elevation of intracellular ROS and Ca^{2+} levels can contribute to LDP-induced apoptotic cell death and HDP-induced necrotic cell death, respectively.

ROLE OF TG2 IN THE CYTOTOXIC RESPONSES TO LDP AND HDP

To investigate the possible roles of TG2 in the cytotoxic responses to LDP and HDP, we initially studied changes in TG2 activity after LDP and HDP. As shown in Figure 4A, LDP elevated TG2 activity by approximately twofold over control levels, and HDP induced a greater stimulation of TG2 (approximately 3.5-fold) than LDP. However, expression level of TG2 was not altered by LDT or HDT
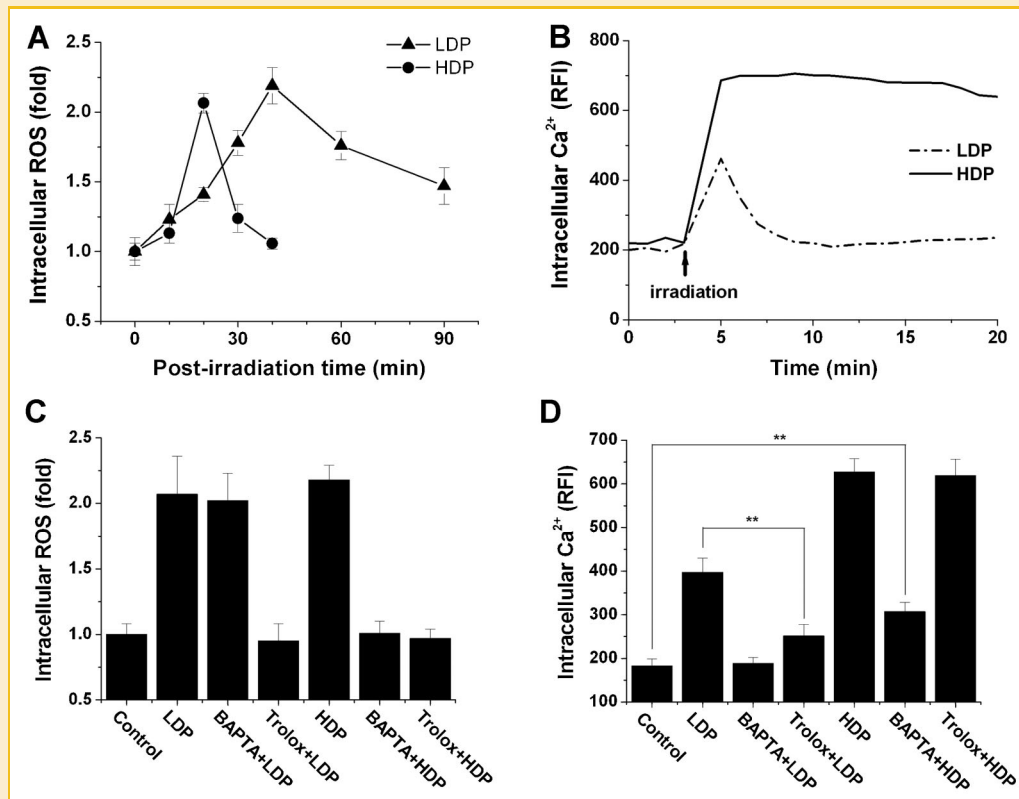
Fig. 3. Changes in intracellular ROS and Ca^{2+} levels induced by LDP and HDP. AGS cells grown on round coverslips were loaded with DH-II-24 for 12 h. Cells were then irradiated in the absence or the presence of 10 μM BAPTA-AM (BAPTA) and 5 mM Trolox, and intracellular ROS and Ca^{2+} levels were determined as described in the Materials and Methods section. A: Time-course changes in the levels of intracellular ROS induced by LDP and HDP. B: Real-time changes in intracellular Ca^{2+} levels induced by LDP and HDP. Each trace is from a single cell representative of at least three independent experiments. C and D: Effect of BAPTA-AM and Trolox on changes in intracellular ROS and Ca^{2+} levels induced by LDP and HDP. Values in graphs represent means $\pm$ S.D. from three independent experiments. $^{**}P < 0.01$.

(data not shown). The greater activation of TG2 by HDP can be explained by the higher and prolonged elevation of intracellular Ca^{2+} levels induced by HDP. Activation of TG2 by LDP and HDP was largely inhibited by Trolox or BAPTA-AM, indicating that increases in intracellular ROS and Ca^{2+} levels are required for both the LDP- and HDP-induced activation of TG2. Next, we studied the possible roles of intracellular ROS and Ca^{2+} levels in cell death caused by LDP or HDP using Trolox and BAPTA-AM (Fig. 4B). LDP decreased cell viability by 50% relative to the control level; however, treatment with either DH-II-24 alone or light alone had little effect on cell viability (Fig. 2A). The LDP-induced decrease of cell viability was largely prevented by Trolox and partially prevented by BAPTA-AM, demonstrating that intracellular ROS rather than intracellular Ca^{2+} are a major mediator in the cytotoxic response to LDP (Fig. 4B). In contrast, the HDP-induced decrease of cell viability was noticeably inhibited by BAPTA-AM and less significantly inhibited by Trolox, supporting that an overload of intracellular Ca^{2+}, at least in part, played a role in the response to HDP (Fig. 4B). However, BAPTA-AM in HDP could not largely inhibit the decrease of cell viability, as observed for Trolox in LDP, and this partial effect might be explained by the partial inhibition of the HDP-induced prolonged elevation of intracellular Ca^{2+} levels by BAPTA-AM (Fig. 3D).

The direct role of TG2 in the PDT-induced death of AGS cells was investigated using TG2-siRNA. Transfection with TG2-siRNA considerably suppressed the expression level of TG2, whereas the expression of β-actin remained unchanged (Fig. 4A Inset). As expected, the elevation of TG2 activity induced by both LDP and HDP was significantly suppressed by transfection with TG2-siRNA (Fig. 4A). TG2-siRNA significantly inhibited the LDP-induced decrease in cell viability; however, it showed no significant effect on HDP-induced cell death (Fig. 4B). In addition, TG2-siRNA prevented the apoptotic cell death caused by LDP, whereas the siRNA did not change the necrotic cell death induced by HDP (data not shown). Thus, we conclude that TG2 plays an essential role in the apoptotic cell death induced by LDP, but TG2 is not critical for the necrotic cell death caused by HDP.

DIFFERENTIAL CYTOTOXIC RESPONSES TO LDP AND HDP IN HUMAN BLADDER CARCINOMA CELLS

To further explore a broad relevance of the preceding results, we investigated the cytotoxic responses to LDP and HDP in human bladder carcinoma J82 cells, which showed a similar uptake of DH-II-24 compared to AGS cells (data not shown). Initially, we examined the mode of cell death by the DiOC$_6$ and PI
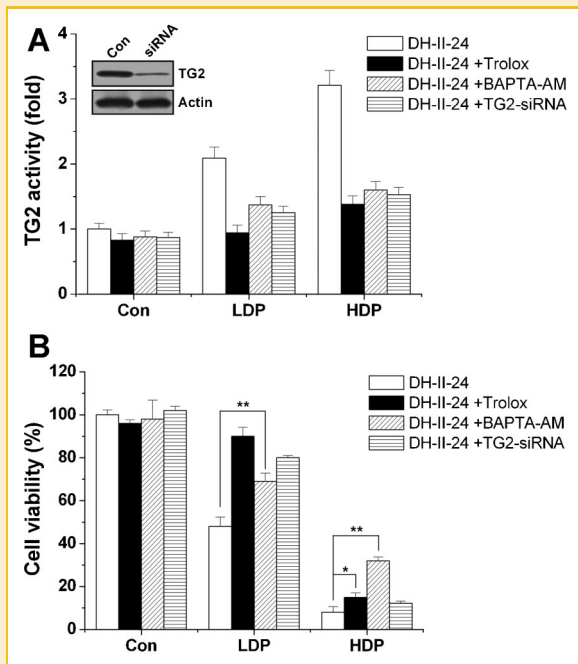
Fig. 4. Role of TG2 in cytotoxic events induced by LDP and HDP. AGS cells were transfected with 200 nM human TG2–siRNA and loaded with DH–II–24 for 12 h. The cells were incubated with 1 mM 5–(biotinamido)pentylamine for 1 h and irradiated. In situ TG2 activity and cell viability were determined as described in the Materials and Methods section. A: Inhibitory effects of 5 mM Trolox, 10 μM BAPTA–AM, and TG2–siRNA on the activation of in situ TG2 by LDP and HDP. B: Effect of various suppressors on the decrease in cell viability. Values in graphs represent means ± S.D. from three independent experiments. $^*P < 0.05$, $^{**}P < 0.01$.

double-staining assay. LDP-treated cells were predominantly distributed in the apoptotic population, whereas HDP-treated cells were highly in the necrotic population, demonstrating that LDP and HDP induced apoptotic and necrotic death of J82 cells, respectively (Fig. 5A). Then, we investigated changes in intracellular ROS and Ca^{2+} levels in responses to the two doses of PDT. LDP and HDP induced significant elevation in levels of intracellular ROS and Ca^{2+}, and their reciprocal roles are shown in Figure 5B and C. Intracellular ROS production contributed to the elevation of intracellular Ca^{2+} level in response to LDP, whereas the elevation of Ca^{2+} resulted in the production of ROS by HDP.

Next, we studied the possible roles of intracellular ROS and Ca^{2+}, and TG2 in cell death caused by LDP and HDP using Trolox, BAPTA-AM, and cystamine, a TGase inhibitor (Fig. 5D). The inhibitors prevented the activation of TG2 by the two doses of PDT (data not shown). The LDP-induced decrease of cell viability was largely blocked by Trolox and cystamine, and partially blocked by BAPTA-AM, thus suggesting a major role of intracellular ROS and TG2 activation rather than intracellular Ca^{2+} in the cytotoxic response to LDP. In contrast, the HDP-induced decrease of cell viability was noticeably reversed only by BAPTA-AM, supporting that an overload of intracellular Ca^{2+}, at least in part, played a role in the cytotoxic response to HDP.

DISCUSSION

PDT is a therapeutic modality that requires the selective uptake of a photosensitizer by tumor cells, followed by irradiation with visible light of an appropriate wavelength that is absorbed by the photosensitizer [Triesscheijn et al., 2006]. Activation of the photosensitizer leads to the conversion of molecular oxygen to various ROS, which ultimately leads to cell death [Buytaert et al., 2007].

Since the balance between apoptosis and necrosis appears to be dependent on several parameters such as cell type, the nature and subcellular localization of photosensitizers, and PDT dose (light dose and photosensitizer concentration) [Piette et al., 2003], we initially determined a suitable PDT dose to stimulate apoptosis or necrosis through cell viability assay at 24 h after irradiation (Table I). Following PDT_{ED50}, approximately 70% of cells were positive for Annexin V. However, PDT_{ED90} displayed PI-positive cells with over 85%, even though about 40% of cells were positive for Annexin V. With PDT_{ED90}, over 20% of cells were co-stained with Annexin V and PI, suggesting the late apoptosis. Moreover, positive cells for PI (over 90%) were predominant to those for Annexin V in PDT_{ED95} (Table I). These data indicate the switch from apoptotic cell death to necrotic cell death in a PDT dose-dependent manner.

To demonstrate the PDT dose-dependent cytotoxic events, we then applied two different doses of PDTs (LDT and HDP) to cancer cells. LDP decreased cell viability by apoptotic death via the TG2/caspase-dependent signaling pathway, coupled with the production of intracellular ROS, which contributed to the elevation of intracellular Ca^{2+} levels (Fig. 6 Left). HDP induced a decrease in cell viability by necrotic death that resulted from an enormous and prolonged increase in intracellular Ca^{2+} levels, which might be directly responsible for the fate of cells. This massive elevation of intracellular Ca^{2+} levels was accompanied by the strong activation of TG2; however, this activation did not contribute to the necrotic death of cancer cells (Fig. 6 Right). Thus, the intracellular Ca^{2+} overload induced by HDP may stimulate not only TG2 but also several proteases such as phospholipase A2, calpains, cathepsins that are implicated in triggering necrosis [Proskuryakov et al., 2003].

While the development of ideal photosensitizers has been continuously considered with improved PDT, chlorin-based photosensitizers including DH-II-24 are especially beneficial in preclinical and clinical PDT for cancer. The antitumor effect of PDT consisting of DH-II-24 was reported using xenograft tumor models [Lim et al., 2009]. DH-II-24 exhibited dominant absorption in the 666-nm region, a longer wavelength than the absorption wavelength of Photofrin, and DH-II-24 was rapidly distributed and cleared across the entire body in mice. DH-II-24-mediated PDT has been reported to induce effective tumor destruction and vascular damage with minimal damage to surrounding normal tissues, suggesting that it can serve as a minimally invasive therapeutic modality for the clinical treatment of cancer [Lim et al., 2009]. In this study, DH-II-24 was taken up by cancer cells in a dose-dependent manner and accumulated predominantly in the ER, but also in the mitochondria and lysosomes. Thus, DH-II-24 would be an effective photosensitizer that can provide various effects in cytotoxic events stimulated by PDT, as the intracellular targets of different therapies can vary.
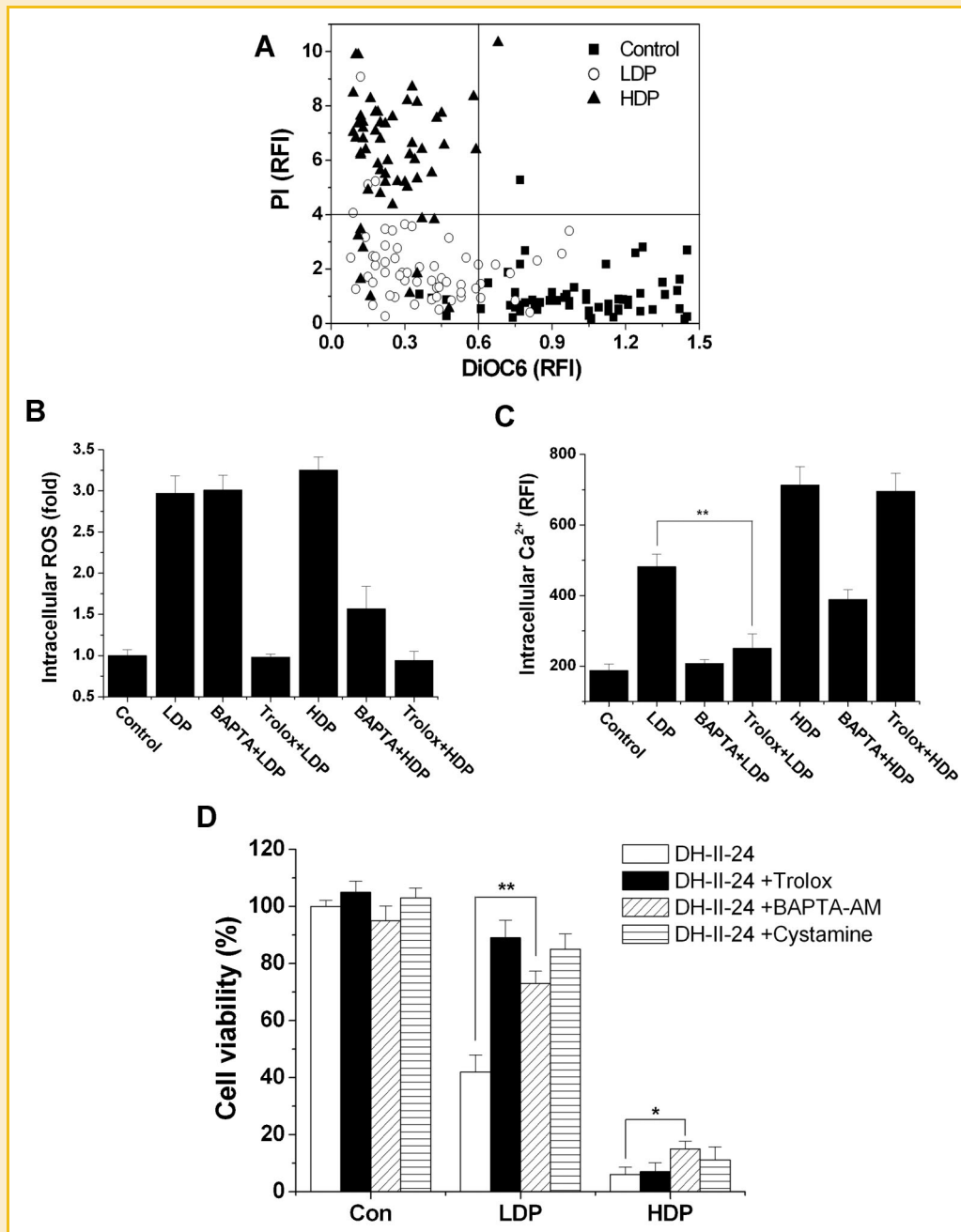
Fig. 5. Differential cytotoxic effects to LDP and HDP in J82 cells. Cells were loaded with 1 or 5 μg/ml DH–II–24 for 12 h and irradiated for 60 or 90 s for LDP and HDP, respectively, in the absence or the presence of 10 μM BAPTA–AM (BAPTA), 5 mM Trolox, and 100 μM cystamine. The mode of cell death, intracellular ROS, Ca^{2+}, and cell viability were determined as described in the Materials and Methods section. A: Cells were stained with DiOC$_6$ and PI, and the fluorescence intensity was measured by processing images at the single–cell level using confocal microscopy. B and C: Effect of BAPTA–AM and Trolox on changes in intracellular ROS and Ca^{2+} levels induced by LDP and HDP. $^{**}P < 0.01$. D: Effect of various suppressors on the decrease in cell viability. Values in graphs represent means ± S.D. from three independent experiments. $^{*}P < 0.05$, $^{**}P < 0.01$.

ROS induced by oxidative stress and intracellular Ca^{2+} act as intracellular messengers to regulate cell signaling that leads to cell death [Ermak and Davies, 2002]. A number of studies suggested that intracellular ROS and Ca^{2+} can function as early mediators in the induction of apoptosis or necrosis [Festjens et al., 2006; Zong and Thompson, 2006] and also in PDT [Almeida et al., 2004; Buytaert et al., 2007; Copley et al., 2008]. Moreover, excessive production of ROS and Ca^{2+} overload may be decisive in promoting necrosis rather than apoptosis [Zong and Thompson, 2006; Buytaert et al., 2007]. We found that LDP induced the production of intracellular ROS that was sustained for at least 90 min after irradiation, whereas HDP instantly induced intracellular ROS production followed by a prompt decrease to the basal level, although similar levels (approximately twofold) of intracellular ROS were produced at

TABLE I. Comparative Analysis of Cell Viability, Annexin V-Positive Cells, and PI-Positive Cells in Various PDT Doses

PDT dose[a]	Assay values (mean ± S.D.)		
	Cell viability (%)	Annexin V-positive cells (%)	PI-positive cells (%)
PDT$_{ED50}$	47.25 ± 3.67	72.65 ± 7.85	8.94 ± 2.41
PDT$_{ED90}$	13.38 ± 3.64	38.32 ± 6.05	87.65 ± 5.69
PDT$_{ED95}$	6.14 ± 2.62	3.54 ± 0.76	93.65 ± 3.47

[a]PDT dose was determined based on cytotoxic effect of PDT with DH-II-24 by cell viability assay. Cell viability was determined at 24 h after irradiation. PDT$_{ED50}$: 1 µg/ml DH-II-24, 87 mJ/cm^2 light dose; PDT$_{ED90}$: 5 µg/ml DH-II-24, 87 mJ/cm^2 light dose; PDT$_{ED95}$: 5 µg/ml DH-II-24, 130.5 mJ/cm^2 light dose. Apoptotic or necrotic cells were identified by examining positive cells for FITC-Annexin V/PI by confocal microscopy. Briefly, AGS cells grown on round coverslips were loaded with DH-II-24 for 12 h and irradiated. The cells were co-stained with FITC-Annexin V (20-fold dilution with 1 × binding buffer) and 10 µg/ml PI without fixation at room temperature for 15 min, using Annexin V-FITC apoptosis detection kit I according to the manufacturer's instructions (BD Biosciences Pharmingen). For quantification of apoptosis or necrosis, at least 300 cells from each sample were examined and the percentage of positive cells for Annexin V or PI was calculated. Values in graphs represent mean ± S.D. from three independent experiments.
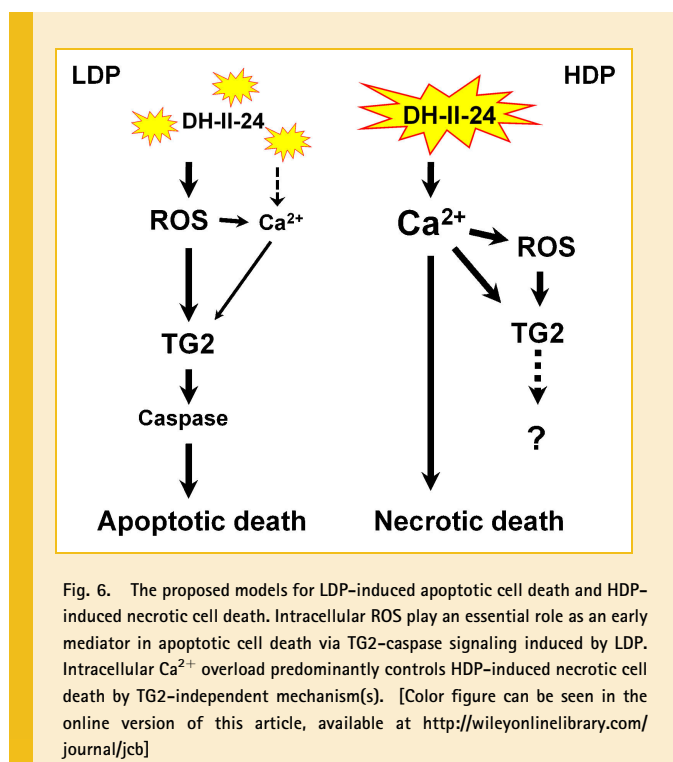

Fig. 6. The proposed models for LDP–induced apoptotic cell death and HDP–induced necrotic cell death. Intracellular ROS play an essential role as an early mediator in apoptotic cell death via TG2–caspase signaling induced by LDP. Intracellular Ca^{2+} overload predominantly controls HDP–induced necrotic cell death by TG2–independent mechanism(s). [Color figure can be seen in the online version of this article, available at http://wileyonlinelibrary.com/journal/jcb]

the different peak times of the two therapies. However, LDP induced a transient increase in intracellular Ca^{2+} levels, whereas HDP caused an enormous and prolonged increase in intracellular Ca^{2+}. These differential cellular responses could be mechanisms for inducing the different modes of cell death caused by LDP and HDP, although the detailed mechanisms by which intracellular ROS and Ca^{2+} regulate cytotoxic events caused by LDP and HDP remain to be elucidated.

ACKNOWLEDGMENTS

REFERENCES

Almeida RD, Manadas BJ, Carvalho AP, Duarte CB. 2004. Intracellular signaling mechanisms in photodynamic therapy. Biochim Biophys Acta 1704:59–86.

Bredell MG, Besic E, Maake C, Walt H. 2010. The application and challenges of clinical PD-PDT in the head and neck region: A short review. J Photochem Photobiol B 101:185–190.

Buytaert E, Callewaert G, Hendrickx N, Scorrano L, Hartmann D, Missiaen L, Vandenheede JR, Heirman I, Grooten J, Agostinis P. 2006. Role of endoplasmic reticulum depletion and multidomain proapoptotic BAX and BAK proteins in shaping cell death after hypericin-mediated photodynamic therapy. FASEB J 20:756–758.

Buytaert E, Dewaele M, Agostinis P. 2007. Molcular effectors of multiple cell death pathways initiated by photodynamic therapy. Biochim Biophys Acta 1776:86–107.

Copley L, van der Watt P, Wirtz KW, Parker MI, Leaner VD. 2008. Photolon, a chlorin e6 derivative, triggers ROS production and light-dependent cell death via necrosis. Int J Biochem Cell Biol 40:227–235.

Douma S, van Laar T, Zevenhoven J, Meuwissen R, van Garderen E, Peeper DS. 2004. Suppression of anoikis and induction of metastasis by the neurotrophic receptor TrkB. Nature 430:1034–1039.

Ermak G, Davies KJA. 2002. Calcium and oxidative stress: From cell signaling to cell death. Mol Immunol 38:713–721.

Festjens N, Vanden BT, Vandenabeele P. 2006. Necrosis, a well-orchestrated form of cell memise: Signaling cascades, important mediators and concomitant immune response. Biochim Biophys Acta 1757:1371–1387.

Fok JY, Mehta K. 2007. Tissue transglutaminase induces the release of apoptosis inducing factor and results in apoptotic death of pancreatic cancer cells. Apoptosis 12:1455–1463.

Griffin M, Casadio R, Bergamini CM. 2002. Transglutaminases: Nature's biological glues. Biochem J 368:377–396.

Kim SW, Lee Z-W, Lee C, Im KS, Ha K-S. 2001. The role of tissue transglutaminase in the germinal vesicle breakdown of mouse oocytes. Biochem Biophys Res Commun 286:229–234.

Kwon M-H, Jung J-W, Jung S-H, Park J-Y, Kim Y-M, Ha K-S. 2009. Quantitative and rapid analysis of transglutaminase activity using protein arrays in mammalian cells. Mol Cell 27:1–10.

Lee Z-W, Kwon S-M, Kim S-W, Yi S-J, Kim Y-M, Ha K-S. 2003. Activation of in situ tissue transglutaminase by intracellular reactice oxygen species. Biochem Biophys Res Commun 305:633–640.

Lim Y-C, Yoo J-O, Kang S-S, Kim Y-M, Ha K-S. 2011. Cellular responses to a chlorin-based photosensitizer DH-II-24 under darkness in human gastric adenocarcinoma AGS cells. Cancer Sci 102:549–556.

Lim Y-C, Yoo J-O, Park D, Kang G, Hwang B-M, Kim Y-M, Ha K-S. 2009. Antitumor effect of photodynamic therapy with chlorin-based photosensitizer DH-II-24 in colorectal carcinoma. Cancer Sci 100:2431–2436.

Lu Z, Tao Y, Zhou Z, Zhang J, Li C, Ou L, Zhao B. 2006. Mitochondrial reactive oxygen species and nitric oxide-mediated cancer cell apoptosis in 2-butylamino-2-demethoxyhypocrellin B photodynamic treatment. Free Radic Biol Med 41:1590–1605.

Mangala LS, Fok JY, Zorrilla-Calancha IR, Verma A, Mehta K. 2007. Tissue transglutaminase expression promotes cell attachment, invasion and survival in breast cancer cells. Oncogene 26:2459–2470.

Nowis D, Makowski M, Stoklosa T, Legat M, Issat T, Golab J. 2005. Direct tumor damage mechanisms of photodynamic therapy. Acta Biochim Polon 52:339–352.

O'Connor AE, Gallagher WM, Byrne AT. 2009. Porphyrin and nonporphyrin photosensitizers in oncology: Preclinical and clinical advances in photodynamic therapy. Photochem Photobiol 85:1053–1074.

Park D, Choi SS, Ha K-S. 2010. Transglutaminase 2: A multi-functional protein in multiple subcellular compartments. Amino Acids 39:619–631.

Piette J, Volanti C, Vantieghem A, Matroule JY, Habraken Y, Agostinis P. 2003. Cell death and growth arrest in response to photodynamic therapy with membrane-bound photosensitizers. Biochem Pharmacol 66:1651–1659.

Proskuryakov SY, Konoplyannikov AG, Gabai VL. 2003. Necrosis: A specific form of programmed cell death? Exp Cell Res 283:1–16.

Robertson CA, Hawkins D, Abrahamse EH. 2009. Photodynamic therapy (PDT): A short review on cellular mechanisms and cancer research applications for PDT. J Photochem Photobiol B 96:1–8.

Robitaille K, Daviau A, Lachance G, Couture JP, Blouin R. 2008. Calphostin C-induced apoptosis is mediated by a tissue transglutaminase-dependent mechanism involving the DLK/JNK signaling pathway. Cell Death Differ 15:1522–1531.

Ruan Q, Quintanilla RA, Johnson GV. 2007. Type 2 transglutaminase differentially modulates striatal cell death in the presence of wild type or mutant huntingtin. J Neurochem 102:25–36.

Sharman WM, Allen CM, van Lier JE. 1999. Photodynamic therapeutics: Basic principles and clinical applications. Drug Discov Today 4:507–517.

Tee AEL, Marshall GM, Liu PY, Xu N, Haber M, Norris MD, Iismaa SE, Liu T. 2010. Opposing effects of two tissue transglutaminase protein isoforms in neuroblastoma cell differentiation. J Biol Chem 285:3561–3567.

Triesscheijn M, Bass P, Schellens JH, Stewart FA. 2006. Photodynamic therapy in oncology. Oncologist 11:1034–1044.

Tucholski J, Johnson GVW. 2002. Tissue transglutaminase differentially modulates apoptosis in a stimuli-dependent manner. J Neurochem 81: 780–791.

Yi S-J, Choi HJ, Yoo J-O, Yuk JS, Jung H-I, Lee S-H, Han J-A, Kim Y-M, Ha K-S. 2004. Arachidonic acid activates tissue transglutaminase and stress fiber formation via intracellular reactive oxygen species. Biochem Biophys Res Commun 325:819–826.

Yoo J-O, Yi S-J, Choi HJ, Kim WJ, Kim Y-M, Han J-A, Ha K-S. 2005. Regulation of tissue transglutaminase by prolonged increase of intracellular Ca^{2+}, but not by initial peak of transient Ca^{2+} increase. Biochem Biophys Res Commun 337:655–662.

Yoo J-O, Lee C-H, Hwang B-M, Kim W-J, Kim Y-M, Ha K-S. 2009. Regulation of intracellular $Ca2+$ in the cytotoxic response to photodynamic therapy with a chlorin-based photosensitizer. J Porphyr Phthalocyanines 13:811–817.

Zong WX, Thompson CB. 2006. Necrotic death as a cell fate. Genes Dev 20: 1–15.